Available online at www.sciencedirect.com
SCIENCE DIRECT
Journal of Molecular Structure 735–736 (2005) 375–382
Journal of MOLECULAR STRUCTURE
www.elsevier.com/locate/molstruc

# Molecular alignment and thermal stability of liquid-crystalline phases in binary mixtures of electron donor and acceptor

Sang-Hee Han[a], Hirohisa Yoshida[a], Yoko Nobe[b], Masahiko Fujiwara[b], Junko Kamizori[b], Azusa Kikuchi[b], Fumiyasu Iwahori[b], Jiro Abe[b,*]

[a]*Department of Applied Chemistry, Tokyo Metropolitan University, 1-1 Minami-ohsawa, Hachiohji, Tokyo 192-0397, Japan*
[b]*Department of Chemistry, Aoyama Gakuin University, 5-10-1 Fuchinobe, Sagamihara, Kanagawa 229-8558, Japan*

Received 2 August 2004; revised 27 September 2004; accepted 2 November 2004
Available online 8 December 2004

**Abstract**

The molecular alignment and thermal stability of the mixtures **DA** composed of two different kinds of Schiff base liquid-crystalline materials, **D** with an electron-donating $-N(CH_3)_2$ unit and **A** with an electron-withdrawing–$NO_2$ unit, were investigated by using DSC, POM, XRD, and FT-IR measurements. The mesophases of the mixtures **DA** were more stable and had wider temperature ranges than those of the individual compounds **D** and **A**. The mixture **DA55** (**D**:**A** = 50:50 mol%) on cooling exhibited the most stable liquid-crystalline phases affording the highest $T_{SI}$ (119 °C), the widest temperature range of the smectic phase (46.4 °C) and the highest values of $\Delta S_{SI}$ (26.1 J $K^{-1}$ $mol^{-1}$) among the mixtures **DA** examined. Based on the analysis of the XRD measurements and the temperature dependence on the FT-IR spectra, the molecular packing of the mixture **DA55** was proposed to form a bilayer structure in the smectic A phase, in which the heading group of the compounds **D** and **A** overlapped partially. The induction of the smectic phase and the enhanced thermal stability for the mixtures **DA** would be caused by the intermolecular interaction between the electron donor and acceptor mesogens.


*Keywords:* Binary mixture; Liquid crystal; Charge transfer; Phase transition

## 1. Introduction

The research on the functionalization of liquid crystals (LCs) and the induction of liquid-crystalline phases by mixing of binary components has been intensively investigated in the past decade. For example, electrically conducting LCs are obtained by discotic LC systems with inorganic dopants [1]. The variation of liquid-crystalline phases [2] and also the phase formation from non-liquid-crystalline compounds are the result of the combination of different interactions, i.e. mesogenic and charge transfer (CT) interactions [3]. It is also known that mesophases with a layered structure (smectic) could be induced in a nematic LC through the steric [4], electronic [5] or CT interactions [6]. The thermal stability of the nematic phase caused by mixing of 4-*n*-butyl-*N*-(4′-methoxylbenzylidene)aniline as an electron donor and 4-*n*-pentyl-4′-cyanobiphenyl as an electron acceptor was investigated [7]. For the similar electron donor and acceptor mixtures, the thermal stability and the induction of smectic phases were reported by Matsunaga and co-workers [8,9].

From the viewpoint of the fundamental research and of applications such as photo- and/or electro-functional materials, the electron donor–acceptor interaction is attracting much attention [10,11]. Tetrathiafulvalene-tetracyanoquinodimethane (TTF-TCNQ) is well-known as an electrically conducting organic CT salt, and the relationship between the crystalline structure and conductivity has been studied extensively [12]. In general, the physical properties of the CT compounds are closely related to the geometrical arrangements of the donor and the acceptor in the CT compounds [13]. In order to design and construct the mesogenic CT complexes with fascinating and desirable properties for electrical conductivity, photoconductivity and nonlinear electrical conductivity, it is very essential to

* Corresponding author. Tel./fax: +81 42 759 6225.
*E-mail address:* jiro_abe@chem.aoyama.ac.jp (J. Abe).

0022-2860/$ - see front matter © 2005 Elsevier B.V. All rights reserved.
doi:10.1016/j.molstruc.2004.11.007

characterize their molecular orientations and to understand the relationships between the CT interactions and their geometrical arrangements.

The introduction of molecular orientation promoting a large overlap of π-orbitals between adjacent π-conjugated molecules is one of the promising approaches to improve the photoinduced charge-carrier transfer ability. Based on this viewpoint, we assumed that liquid-crystalline materials would have some advantages, because they can be obtained as high quality thin films with a high degree of molecular orientation. Therefore, the utilization of the photoinduced charge-carrier transporting ability and the self-organized mesophase in the binary system is a promising possibility for the application in photo-electronic devices as liquid-crystalline semiconductors and solar cells.

Our research interest is on the examination of the applicability of mesophases induced by molecular complexing with the aim of the fabrication of dynamically functional material as photovoltaic devices. We synthesized mesophases taking into account the similar one employed by Matsunaga and co-workers in binary system [14]. In the literature, the electronic absorption band being assignable to the CT band within the donor–acceptor pair was observed in *N*-(4-ethoxybenzylidene)-4-(dimethylamino)aniline and *N*-(4-ethoxybenzylidene)-4-nitroaniline system. However, the details of the CT band in other systems and the molecular arrangements of the donor–acceptor pair in smectic phases are still unexplored.

In this paper, we describe the thermal stability on the phase transition behavior of the mixtures **DA** of *N*-(4-*n*-hexyloxybenzylidene)-4-(dimethylamino)aniline (**D**) and *N*-(4-*n*-hexyloxybenzylidene)-4-nitroaniline (**A**). For further investigation of the induction of smectic phases in the binary system [14], we would like to describe the molecular arrangements in the smectic phase induced by the intermolecular interaction between the electron-donating and -withdrawing mesogens. The mixtures **DA** will be characterized by optical microscope observation, differential scanning calorimeter, X-ray diffraction measurements, and FT-IR spectra.

## 2. Experimental section

### 2.1. Reagents and preparation

4-Nitroaniline, 4-hydroxybenzaldehyde, *N*,*N*-dimethyl-1,4-phenylenediamine and 1-bromohexane (Tokyo Kasei Kogyo Co., Ltd) were used without further purification. 4-[(4-dimethylaminophenylimino)methyl]phenol, 4-[(4-nitrophenylimino)methyl]phenol, *N*-(4-*n*-hexyloxybenzylidene)-4-(dimethylamino)aniline and *N*-(4-*n*-hexyloxybenzylidene)-4-nitroaniline were prepared according to the procedure shown in Scheme 1.

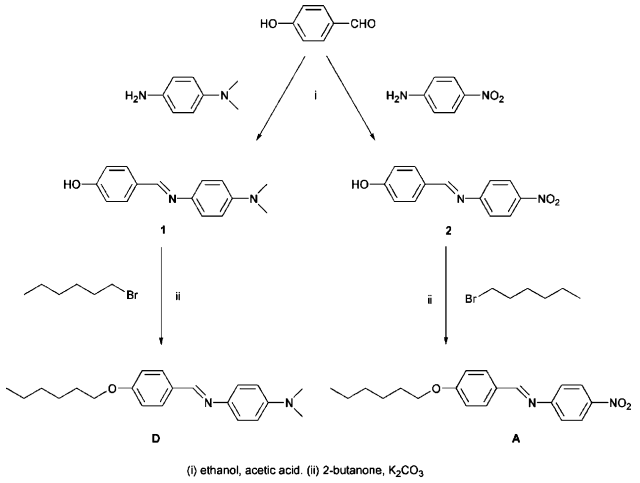


Scheme 1. Synthetic procedures of the compounds **D** and **A**.

### 2.2. 4-[(4-dimethylaminophenylimino)methyl]phenol (*1*)

A mixture of *N*,*N*-dimethyl-1,4-phenylenediamine (1.1 g, 8.2 mmol), 4-hydroxybenzaldehyde (1.0 g, 8.2 mmol) and four drops of acetic acid were added to ethanol (50 ml) in 100 ml two-necked round-bottom flask equipped with a reflux condenser. The reaction mixture was stirred in oil bath at 85 °C. The reaction was monitored by TLC ($CHCl_3$:hexane, 9:1). After stirring for 4 h, the solvent was evaporated under reduced pressure to near dryness. The crude product was purified by recrystallization from ethanol. The light yellow solid of **1** was obtained (1.4 g, 5.9 mmol, yield: 72%). $^1$H NMR (500 MHz, DMSO-$d_6$) δ: 9.97 (s, 1H, OH), 8.47 (s, 1H, –CH=N–), 7.71 (d, 2H, H–Ar), 7.18 (d, 2H, H–Ar), 6.84 (d, 2H, H–Ar), 6.74 (d, 2H, H–Ar) and 2.90 (s, 6H, N–$(CH_3)_2$).

### 2.3. 4-[(4-nitrophenylimino)methyl]phenol (*2*)

A mixture of 4-nitroaniline (1.0 g, 7.2 mmol), 4-hydroxybenzaldehyde (0.9 g, 7.2 mmol) and *p*-toluenesulfonic acid monohydrate (0.013 g, 0.070 mmol) were added to xylene (60 ml) in 100 ml two-necked round-bottom flask equipped with a reflux condenser. The reaction mixture was stirred in oil bath at 150 °C. The reaction was monitored by TLC ($CHCl_3$:hexane, 9:1). After stirring for 7 h, the solvent was evaporated under reduced pressure to near dryness. The crude product was purified by recrystallization from ethanol. The light yellow solid of **2** was obtained (1.0 g, 4.2 mmol, yield: 58%). $^1$H NMR (500 MHz, DMSO-$d_6$) δ: 10.29 (s, 1H, OH), 8.50 (s, 1H, –CH=N–), 8.24 (d, 2H, H–Ar), 7.81 (d, 2H, H–Ar), 7.37 (d, 2H, H–Ar) and 6.90 (d, 2H, H–Ar).

### 2.4. N-(4-n-hexyloxybenzylidene)-4-(dimethylamino)aniline (*D*)

A mixture of compound **1** (1.0 g, 4.2 mmol), 1-bromohexane (2.1 g, 12.7 mmol) and $K_2CO_3$ (1.8 g,

12.7 mmol) were added to 2-butanone (50 ml) in 100 ml two-necked round-bottom flask equipped with a reflux condenser. The reaction mixture was stirred in oil bath at 150 °C. The reaction was monitored by TLC ($CHCl_3$: hexane, 9:1). After stirring for 5 h, the resultant yellow solution was filtered, and the solvent was removed under reduced pressure. The crude product was purified by recrystallization from ethanol. The light yellow solid of **D** was obtained (1.1 g, 3.3 mmol, yield: 78%). $^1$H NMR (500 MHz, DMSO-$d_6$) δ: 8.52 (s, 1H, –CH=N–), 7.80 (d, 2H, H–Ar), 7.20 (d, 2H, H–Ar), 7.01 (d, 2H, H–Ar), 6.74 (d, 2H, H–Ar), 4.01 (t, 2H, –O–$CH_2$–), 2.90 (s, 6H, N–$(CH_3)_2$), 1.72 (m, 2H, –O–$CH_2$–C**H**$_2$–), 1.29–1.43 (m, 6H, –$(CH_2)_3$–) and 0.87 (t, 3H, –$CH_3$). Anal. calcd for $C_{21}H_{28}N_2O$: C 77.74, H 8.70, N 8.63; found: C 77.75, H 8.71, N 8.74.

### 2.5. N-(4-n-hexyloxybenzylidene)-4-nitroaniline (*A*)

A mixture of compound **2** (0.8 g, 3.3 mmol), 1-bromohexane (1.6 g, 9.9 mmol) and $K_2CO_3$ (1.4 g, 9.9 mmol) were added to 50 ml of 2-butanone in 100 ml two-necked round-bottom flask equipped with a reflux condenser. The reaction mixture was stirred in oil bath at 150 °C. The reaction was monitored by TLC ($CHCl_3$:hexane, 9:1). After stirring for 5 h, the resultant yellow solution was filtered, and the solvent was removed under reduced pressure. The crude product was purified by recrystallization from ethanol. The light yellow crystalline solids of **A** was obtained (0.8 g, 2.5 mmol, yield: 76%). $^1$H NMR (500 MHz, DMSO-$d_6$) δ: 8.56 (s, 1H, –CH=N–), 8.25 (d, 2H, H–Ar), 7.91 (d, 2H, H–Ar), 7.39 (d, 2H, H–Ar), 7.08 (d, 2H, H–Ar), 4.05 (t, 2H, –O–$CH_2$–), 1.73 (m, 2H, –O–C**H**$_2$–$CH_2$–), 1.29–1.43 (m, 6H, –$(CH_2)_3$–) and 0.87 (t, 3H, –$CH_3$). Anal. calcd for $C_{19}H_{22}N_2O_3$: C 69.92, H 6.79, N 8.58; found: C 69.85, H 6.82, N 8.65.

### 2.6. Physical measurements

Molecular alignment and thermal stability on the phase transition behavior of the compounds **D**, **A** and the mixtures **DA** were evaluated by differential scanning calorimeter (DSC: Seiko I&E DSC-6200), polarizing optical microscopy (POM; Olympus Model BX-51), FT-IR spectrometer and X-ray diffractometer. During the VT (variable temperature)-IR, melting-, and clearing-point measurements on polarized microscopy analyses, temperature was controlled using a hot stage (Imoto) with an accuracy of ± 0.1 °C. The heating rate for all variable temperature measurements was 5 °C min$^{-1}$.

The thermodynamic properties for phase transition of the compounds **D**, **A**, and the mixtures **DA** were explored by means of DSC. About 5 mg of the sample completely dried was placed in aluminum sample pan and sealed. Measurements were carried out in the temperature range from 30 to 130 °C. The phase transition temperature was taken as a peak top, and the enthalpy change was determined from the peak area. In order to check the reproducibility, the measurements were done in quadruplicate for the same sample. The reproducibility of the phase transition temperature and the enthalpy was ±0.3 °C and ±7%, respectively. The entropy change was calculated by assuming that the transition is sufficiently reversible.

The XRD measurements were performed on a MXP-18 (MAC Science Co., Ltd) diffractometer using Cu K$\alpha_1$ radiation ($\lambda = 0.15405$ nm). Infrared spectra were measured using a FT-IR spectrometer (Shimadzu FTIR-8400S) operating at 2 cm$^{-1}$ resolution with an unpolarized beam striking the sample at normal incidence. The transparent KBr disks obtained (10 mm in diameter and 2 mm in thickness) were used for the VT-IR measurements.

## 3. Results and discussion

Fig. 1 shows typical DSC thermograms observed for the compounds **D**, **A** and the mixtures **DA** in the second heating and cooling scanning. The measured enthalpy ($\Delta H_{SI}$) and entropy ($\Delta S_{SI}$) changes on the second heating and cooling for the compounds are summarized in Table 1. On the second cooling scanning, the compounds **D** and **A** exhibit only monotropic nematic phases (**N**) over relatively narrow temperature range from 81.3 to 93.1 °C and from 75.6 to 79.5 °C, respectively. However, all of the mixtures **DA** on the heating and cooling scanning display the smectic phase (**S**) as identified by POM and XRD measurements. It should be assumed that intermolecular interaction between the electron donor and acceptor mesogens is responsible for the formation of smectic phase. This is not surprising in view of the previous studies with other similar compounds [14], but it is significant to understand the nature and degree of interactions between two different components. Additionally, the mixture **DA55** shows the two-phase region with coexisting the crystalline phase and smectic phase from 74.1 to 95.9 °C on heating and from 59.3 to 72.6 °C on cooling. Also, as shown in Table 1, the measured enthalpy and entropy changes at the smectic to isotropic phase transition on heating of the mixture **DA55** were 10.6 and 27.1 J K$^{-1}$ mol$^{-1}$, respectively. These results clearly indicate that the mixtures **DA28** and **DA55** show a stable liquid-crystalline phase and a simple phase transition behavior. In particular, the mixture **DA55** on cooling exhibits the most stable liquid-crystalline phases as evidenced by the highest $T_{SI}$ (119 °C), the widest temperature range of the smectic phase (46.4 °C) and the highest values of $\Delta S_{SI}$ (26.1 J K$^{-1}$ mol$^{-1}$) among the mixtures **DA** examined.

Fig. 2 displays the corresponding phase diagrams of the mixtures **DA** for the content of the compound **D** on heating and cooling cycle. The mixtures **DA** exhibit the smectic phase when the content of the compound **D** was in the range between 20 and 80 mol%, while the smectic phase was not appeared in the individual compounds **D** and **A**. The mixture

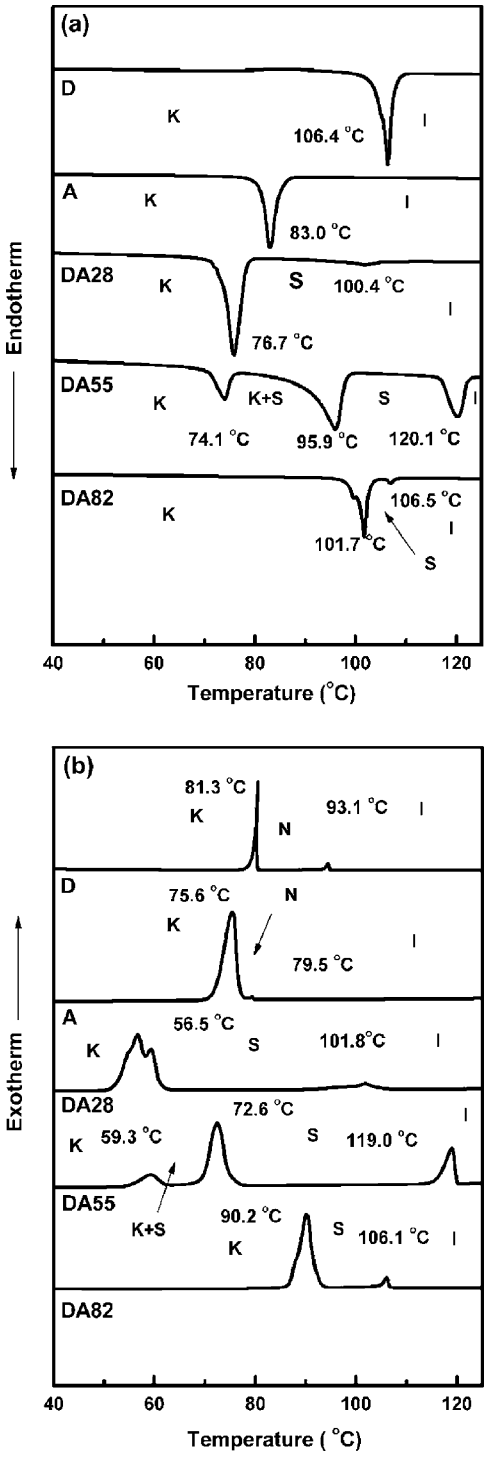


Fig. 1. DSC thermograms observed for the compounds **D**, **A**, and the mixtures **DA**: (a) the second heating scan; (b) the second cooling scan. Abbreviations: **K**, crystalline; **S**, smectic phase; **N**, nematic phase; **I**, isotropic phase.

**DA55** exhibits the smectic phase in the considerably wide temperature range from 72.6 to 119 °C. Interestingly, the temperature range of the induced smectic phase in the mixture **DA28** is much wider than that in the mixture **DA82** on cooling cycle. Thus, the appearance of mesophase in the mixtures **DA** may be tuned from the smectic phase to the nematic phase due to the variation of electron donor–acceptor interaction. Bogojawlensky and co-workers studied a number of binary systems in which one or both compounds are also mesomorphic and demonstrated that in many cases the transition curves separating the isotropic liquids and mesophases in the phase diagrams are nearly linear [15,16]. When the interaction between the different component molecules is more attractive than those between identical molecules, the transition curve is expected to become convex upwards. In other words, the mesophase in the binary mixture is more stable than that expected from the ideal linear correlation [9]. Both on heating and cooling, the phase transition curve from smectic to isotropic for these mixtures **DA** is seen to have a very curvature. Such an enhancement of the thermal stability of mesophases is in good agreement with the phase diagrams in Fig. 2, although the phase transition behavior of mesophase in the mixtures **DA** is examined at least in the limited compositions chosen.

Fig. 3 shows the optical textures of the compounds **D**, **A** and the mixtures **DA** observed in a sandwiched glass cell. On cooling from the isotropic phase, the compounds **D** and **A** exhibit only the typical Schlieren texture attributable to the nematic phase as shown in Fig. 3(a) and (b). On the contrary, on cooling from isotropic state, the mixtures **DA28** and **DA55** exhibit the focal conic fan textures (Fig. 3(c) and (d)) usually observed for the smectic A phase rather than the broken-fan texture characteristic to the smectic C phase, while the mixture **DA82** shows only the Schlieren texture (Fig. 3e) [17,18]. On the XRD analysis of the mixture **DA82**, however, a sharp peak at $2\theta = 3.53°$ (layer distance = 25.0 Å) attributing to the smectic layering was observed in addition to a broad peak at $2\theta = 19.93°$ (see Table 2 and Fig. 4). These results may suggest that all of the mixtures **DA** have a smectic A phase.

To confirm the assignments of the LC phases and to understand the molecular alignment induced by the electron donor–acceptor interaction, powder XRD measurements were performed with the mixtures **DA** at various temperatures. The structural parameters for the liquid-crystalline phase of the mixtures **DA** determined by the XRD measurements were summarized in Table 2. Fig. 4 shows the comparison of the XRD patterns for the mixtures **DA**. These XRD patterns for the mixtures **DA** below the isotropic transition temperature showed a sharp Bragg peak at small angles and a broad halo at wide angles associated with the smectic character of the mesophases. These diffraction patterns at small angle of the mixtures **DA55** and **DA28** indicate a well-oriented arrangement of the compounds **D** and **A**, which consists of bimolecular layers in the smectic phase. However, the XRD pattern of the mixture **DA82** gives somewhat broad and weak peaks at small angles compared with those of the mixtures **DA28** and **DA55**. It should be assumed that the degree of alignment within the layer of the mixture **DA82** is lower than those of the mixtures **DA55** and **DA28**. The corresponding smectic

Table 1
Thermodynamic characterization for phase transition of the compounds **D**, **A**, and the mixtures **DA**

| Compound designation | **D:A** (mol%)[a] | Heating ( °C)/cooling ( °C)[b] | $\Delta H$ (k J mol$^{-1}$)[c] | $\Delta S$ (J K$^{-1}$ mol$^{-1}$)[c] |
|---|---|---|---|---|
| **D** | 100:0 | **K** 106.4 **I** | | |
| | | **K** 81.3 **N** 93.1 **I** | 3.1 | 8.5 |
| **A** | 0:100 | **K** 83.0 **I** | | |
| | | **K** 75.6 **N** 79.5 **I** | 0.8 | 0.5 |
| **DA28** | 20:80 | **K** 76.7 **S** 100.4 **I** | 3.4 | 9.3 |
| | | **K** 56.5 **S** 101.8 **I** | 4.4 | 11.7 |
| **DA55** | 50:50 | **K** 95.9 **S** 120.1 **I** | 10.6 | 27.1 |
| | | **K** 72.6 **S** 119.0 **I** | 10.2 | 26.1 |
| **DA82** | 80:20 | **K** 101.7 **S** 106.9 **I** | 1.3 | 3.5 |
| | | **K** 90.2 **S** 106.1 **I** | 2.4 | 6.3 |

[a] The ratio of the compounds **D** and **A**.
[b] Transition temperature ( °C) determined by the DSC measurement at a scanning rate of 5 °C/min on the second heating and cooling scans.
[c] Measured by DSC. $\Delta H$, enthalpy change from mesophase to isotropic; $\Delta S$, entropy change from mesophase to isotropic.

layer spacing calculated from the diffraction angle were 26.1 Å ($2\theta = 3.38°$), 24.8 Å ($2\theta = 3.56°$) and 25.0 Å ($2\theta = 3.53°$) for the mixtures **DA28**, **DA55** and **DA82**, respectively. The broad reflections at wide-angles region were approximately 6.7 Å ($2\theta = 13.30°$) and 4.5 Å ($2\theta = 20.18°$), 7.2 Å ($2\theta = 12.33°$) and 4.5 Å ($2\theta = 20.09°$), 6.6 Å ($2\theta = 13.53°$) and 4.5 Å ($2\theta = 19.93°$) for the mixtures **DA28**, **DA55** and **DA82**, respectively. These diffuse scattering halos in wide-angle region observed for the mixtures **DA** are related to an average distance as a consequence of the fluid like ordering of the molten aliphatic chains and rigid parts formed within the smectic layers. Diffuse halos centered around at 4.5 Å for all of the mixtures were tentatively assigned to the mean lateral distance between the alkyl chains. Especially, the origin of the diffuse diffraction peaks from 6.6 to 7.2 Å at wide-angle region may be due to the average lateral distance between two mesogenic cores. In Fig. 4(b), the molecular lengths estimated by the MM2 parameters were approximately 19.6 and 20.5 Å for the compounds **D** and **A**, respectively. Thus, on the basis of the results for these XRD measurements and the fully extended molecular conformations, the proposed model of a smectic layer structure for the mixture **DA55** could be illustrated in the Fig. 4(c). The molecular packing of the mixture **DA55** may have a bilayer structure in the smectic A phase, in which alkyl chains are highly interdigitated and heading groups of the compounds **D** and **A** overlapped partially.

Fig. 5 shows the temperature dependence for small angle XRD patterns of the mixture **DA55** on the second cooling. The measurements were carried out over a temperature range from 48 to 124 °C at an increment of 10 °C. The first and second Bragg peaks for the mixture **DA55** were observed at a temperature of 114, 95 and 85 °C. The Bragg angle $2\theta$ for small angle peak also maintained constant in the temperature range of the smectic phase. This implies that the same orientation in the smectic A phase is kept uniformly over the temperature range of the mesophase. Two-phase region (K + S) with coexisting the crystalline phase and the smectic phase were clearly observed at 66 and 74 °C.

The direct evidence for the presence of the CT between electron-donating *N*-(4-*n*-hexyloxybenzylidene)-4-(dimethylamino)aniline (**D**) and electron-withdrawing *N*-(4-*n*-hexyloxybenzylidene)-4-nitroaniline (**A**) should be given by the observation of a CT absorption band in an electronic absorption spectrum. Indeed, the appearance of an additional electronic absorption band attributable to the CT transition associated with the electron donor–acceptor pairs was reported for the diffuse reflection spectrum of the mixture of *N*-[4-(dimethylamino)benzylidene]-4-phenetidine and *N*-(4-nitrobenzylidene)-4-phenetidine [14].

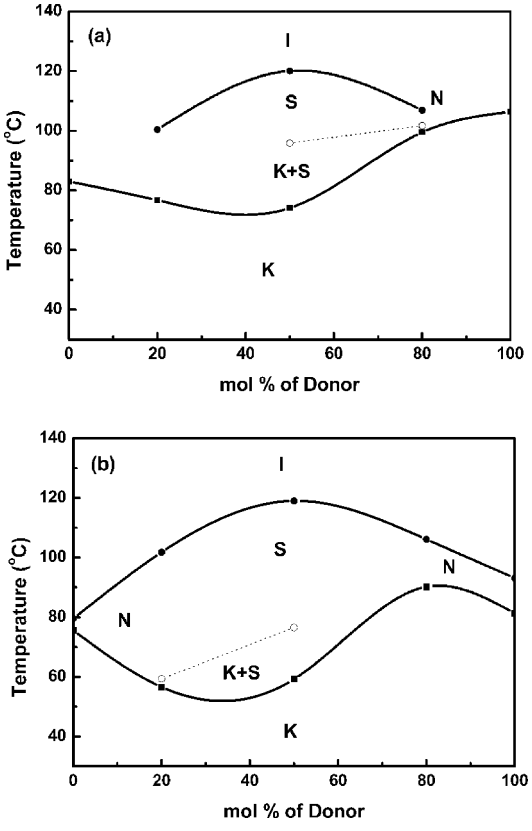


Fig. 2. Binary phase diagrams of the mixtures **DA**: (a) the second heating scan; (b) the second cooling scan.

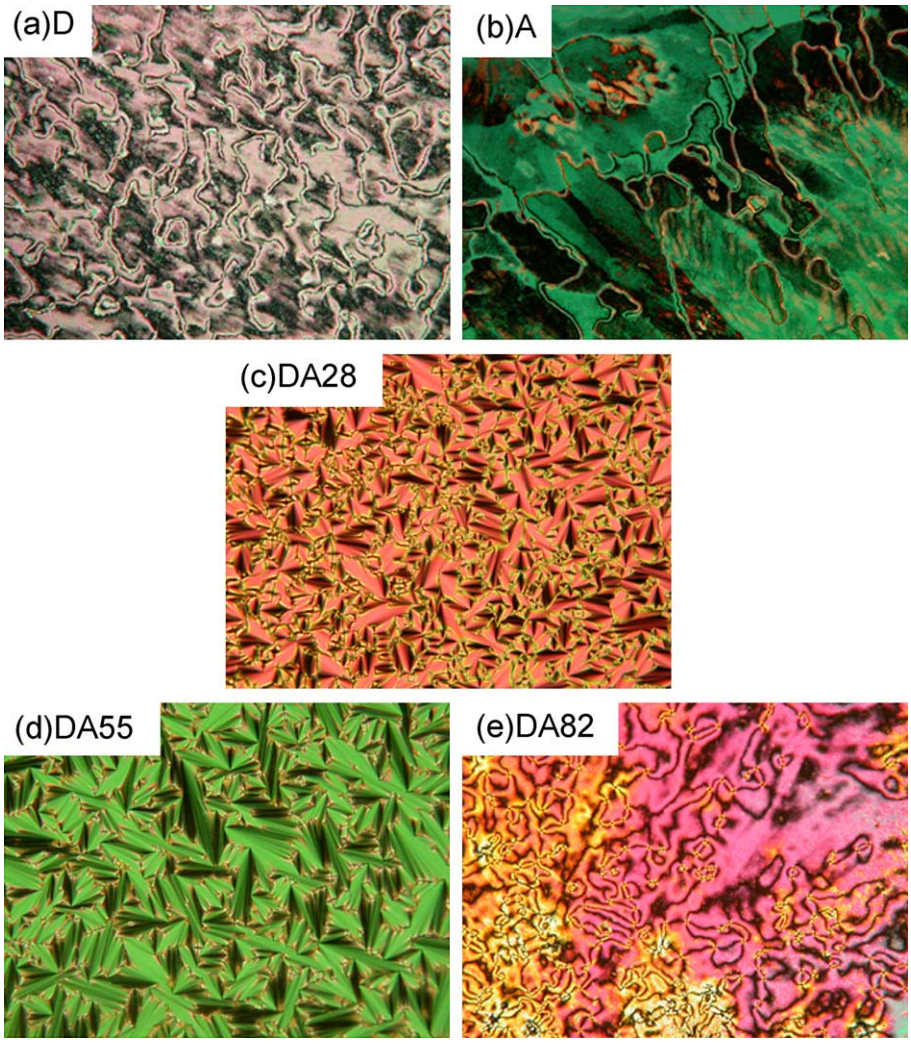


Fig. 3. Polarized optical micrographs for the compounds **D**, **A**, and the mixtures **DA** between crossed polarizers, all of the pictures were obtained upon cooling from the isotropic phase. (a) The mesophase of the compound **D** at 85 °C, (b) the mesophase of the compound **A** at 74 °C, (c) the mesophase of the mixture **DA28** at 88 °C, (d) the mesophase of the mixture **DA55** at 95 °C, (e) the mesophase of the mixture **DA82** at 104 °C.

The color of the binary mixtures **DA** is reddish brown in both solid and liquid-crystalline states, while those of the compounds **D** and **A** are only yellow. The reflection spectrum measured in the mesophases of the mixture **DA55** was shown in Fig. 6 together with those of **D** and **A**. The broad absorption band was observed in the spectral range from 450 to 550 nm. This absorption band was also detected both in solid and isotropic phases. These observations can be considered as the direct evidence for the formation of CT complex in the mixture **DA55** between **D** and **A**. Turning the viewpoint from the changes in electronic structures to the changes in molecular structures induced by the donor–acceptor interaction, we have investigated the temperature dependence on the FT-IR spectra (VT-IR) of the mixture **DA55**. Fig. 7 shows the VT-IR spectra of the mixture **DA55** in a KBr disk on the second cooling. The absorption peaks around 1550–1650 $cm^{-1}$ significantly changed with temperature. These peaks could be assigned to the C=C stretching modes of phenylenes and the C=N stretching mode. Though these spectral changes would imply the changes in the molecular interaction or orientation between adjacent molecules, it is difficult to speculate the changes in the molecular interaction from the IR spectra. Therefore, we have focused on the absorption bands at 1510 and 1340 $cm^{-1}$ in order to obtain the information for the molecular interaction concerning these absorption bands. Strong absorption peaks around at 1510

Table 2
X-ray diffraction data for the mixtures **DA**

| Compound designation | $d_v$ (Å)[a] | $d_{la}$ (Å)[b] | $d_{lb}$ (Å)[b] | Temperature (°C) |
|---|---|---|---|---|
| **DA28** | 26.1 | 6.7 | 4.5 | 76 |
| **DA55** | 24.8 | 7.2 | 4.5 | 100 |
| **DA82** | 25.0 | 6.6 | 4.5 | 95 |

[a] Vertical interlayer spacing.
[b] Average lateral distance of the molten aliphatic chains and rigid parts between the compounds **D** and **A**.

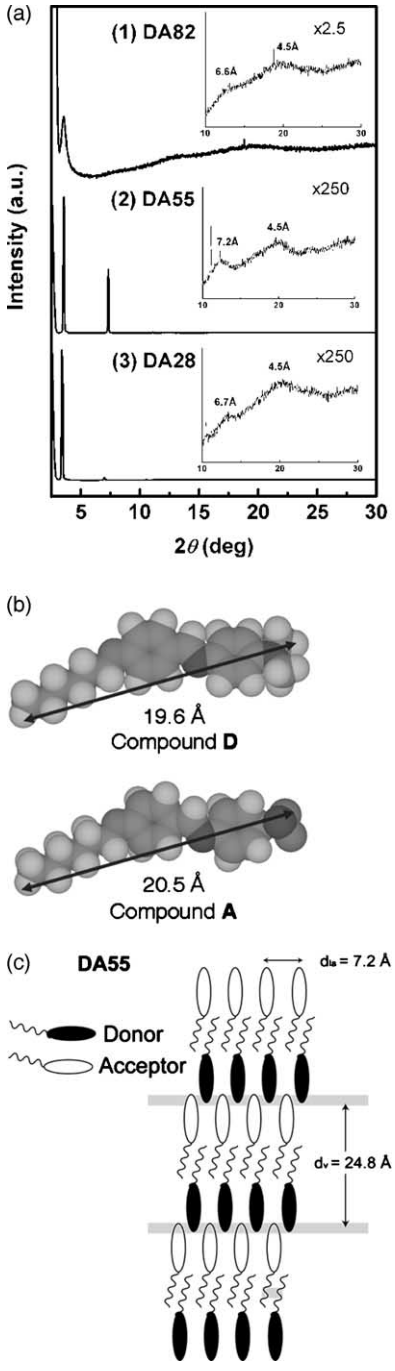


Fig. 4. (a) Powder X-ray diffraction patterns of the mixtures **DA** measured on the second cooling: (1) **DA82** at 95 °C, (2) **DA55** at 100 °C, (3) **DA28** at 76 °C. (b) Minimized energy conformations of the compounds **D**, **A**. (c) Schematic illustration of a proposed mesophase structure in the mixture **DA55**.

and 1340 $cm^{-1}$ could be tentatively assigned to the asymmetric $\nu_{as}(-NO_2)$ and symmetric $\nu_s(-NO_2)$ stretching vibrational modes of **A**, respectively. Both of the peaks show the higher frequency shift with increasing the temperature, indicating the variations in the molecular alignment on the phase transitions. The spectra in the

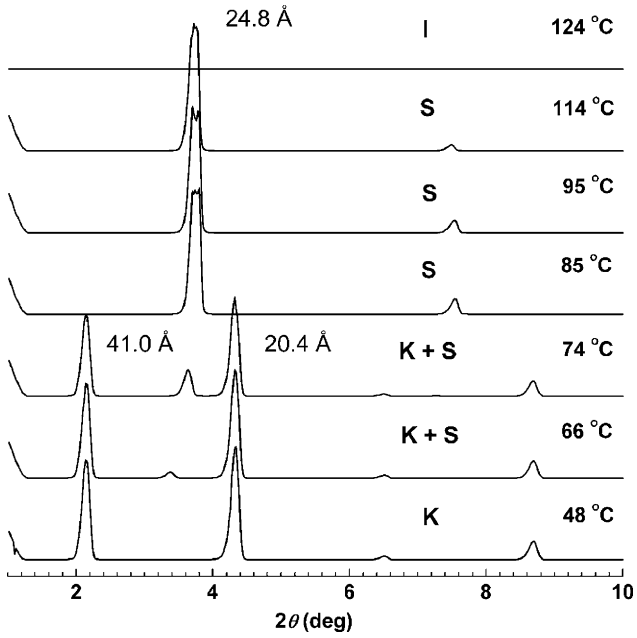


Fig. 5. Temperature dependence of the small angle X-ray diffraction patterns of the mixture **DA55** measured on the second cooling.

smectic phase largely changed compared with those of the crystalline phase. These frequency shifts could be attributable to the increase in the degree of the molecular interaction between **D** and **A** in the smectic phase. However, only the small changes in the spectra could be found in those of the isotropic phase in comparison with those of the smectic phase. These results indicate that the molecular interaction in the smectic phase is also maintained in the isotropic phase. In general, the optical anisotropy are missing in an isotropic phase, the presence of the donor–acceptor interactions in the molecular-scale region in the mixtures **DA55** was suggested.

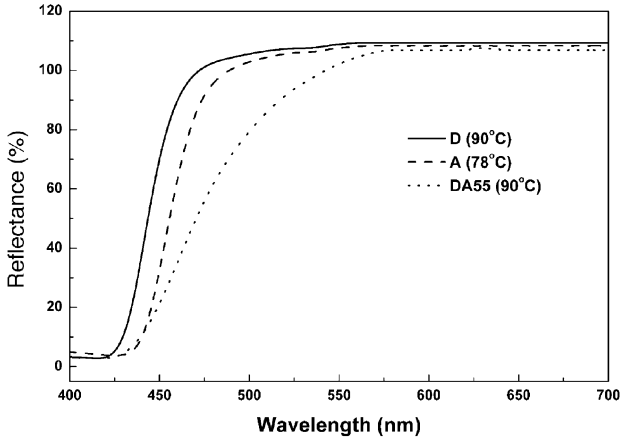


Fig. 6. Reflection spectra of the compounds **D** (solid line), **A** (dash line), and the mixture **DA55** (dot line) in the liquid-crystalline phase.

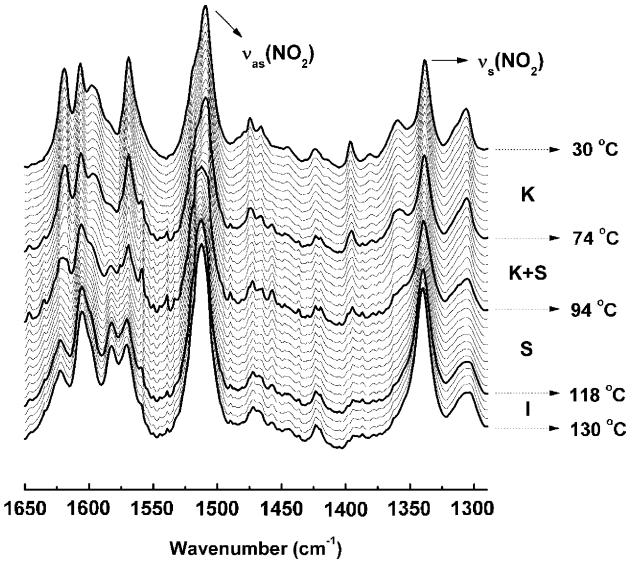


Fig. 7. Temperature dependence of the IR spectra of the mixture **DA55** in a KBr disk measured on the second cooling.

## 4. Conclusion

Schiff base liquid-crystalline *N*-(4-*n*-hexyloxybenzylidene)-4-(dimethylamino)aniline (**D**) and *N*-(4-*n*-hexyloxybenzylidene)-4-nitroaniline (**A**) were prepared, and the molecular alignment and the thermal stability for the binary mixtures **DA** were investigated. Thermodynamic properties indicated that the mixtures **DA** were thermally stable, even though the renowned instability of Schiff base was usually mentioned. The mesophase range of the mixtures **DA** showed a wider temperature range than those of the individual compounds **D** and **A** due to the intermolecular interaction between the electron donor and acceptor groups. X-ray diffraction patterns at small and wide angle for the mixtures **DA** revealed a well-oriented bilayer structure in the smectic A phase, in which heading groups between the compounds **D** and **A** overlapped partially. These mixtures **DA** provided us with a promising possibility for practical application in photo-electronic devices. The optoelectronic properties of binary mixtures **DA** will be discussed elsewhere.

## Acknowledgements

This work was partially supported by a Grant-in-Aid for the 21st Century COE Program (Aoyama Gakuin University) from the Ministry of Education, Culture, Sports, Science and Technology, Japan.

## References

[1] L.Y. Chiang, J.P. Stokes, C.R. Sainya, A.N. Bloch, Mol. Cryst. Liq. Cryst. 125 (1985) 279; J. van Keulen, T.W. Warmerdam, R.J.M. Nolte, W. Drenth, Rec. Trav. Chim. Pays.-Bas Belg. 106 (1987) 534; N. Boden, R.J. Bushby, J. Clements, M.V. Jesudason, P.F. Knowles, G. Williams, Chem. Phys. Lett. 152 (1988) 94.
[2] F.D. Saeva, G.A. Reynolds, L. Kaszczuk, J. Am. Chem. Soc. 104 (1982) 3524.
[3] H. Bengs, M. Ebert, O. Karthaus, B. Kohne, K. Praefcke, H. Ringsdorf, G.H. Wendorff, R. Wustefeld, Adv. Mater. 2 (1990) 141.
[4] W.H. de Jeu, L. Longa, D. Demus, J. Chem. Phys. 84 (1986) 6410; B. Ziemnicha, A. de Vries, I.W. Doane, S.L. Arora, Mol. Cryst. Liq. Cryst. 132 (1986) 289; M.E. Neubert, K. Leung, W.A. Saupe, Mol. Cryst. Liq. Cryst. 134 (1986) 283; C.S. Oh, Mol. Cryst. Liq. Cryst. 41 (1977) 1.
[5] S. Diele, G. Pelz, W. Weissflog, D. Demus, Mol. Cryst. Liq. Cryst. 3 (1988) 1947.
[6] G. Pelzl, U. Boettger, S. Diele, D. Demus, Cryst. Res. Technol. 22 (1987) 1321; G. Pelzl, M. Novak, W. Weissflog, D. Demus, Demus, Cryst. Res. Technol. 22 (1987) K125.
[7] J.W. Park, C.S. Bak, M.M. Labes, J. Am. Chem. Soc. 97 (1975) 4398.
[8] K. Araya, Y. Matsunaga, Bull. Chem. Soc. Jpn 53 (1980) 989.
[9] K. Araya, Y. Matsunaga, Mol. Cryst. Liq. Cryst. 67 (1981) 153.
[10] N. Koide, S. Ogura, Y. Aoyama, Mol. Cryst. Liq. Cryst. 198 (1991) 323.
[11] W.T. Ford, M. Bautista, M. Zhao, R.J. Reeves, R. Powell, Mol. Cryst. Liq. Cryst. 198 (1991) 351.
[12] R. Yuge, A. Miyazaki, T. Enoki, K. Tamada, F. Nakamura, M. Hara, J. Phys. Chem. B. 196 (2002) 6894.
[13] H.S. Wang, Y. Ozaki, Langmuir 16 (2000) 7070.
[14] K. Araya, Y. Matsunaga, Bull. Chem. Soc. Jpn 53 (1980) 3079.
[15] A. Bogojawlensky, Z. Winogradow, Phys. Chem. 64 (1908) 229.
[16] R. Walter, Ber. 58 (1925) 2303.
[17] D. Demus, L. Richter, Textures of Liquid Crystals, Verlag Chemie, Weinheim, 1978.
[18] G.W. Gray, J.W. Goodby, Smectic Liquid Crystal, Textures and Structures, Leonard Hill, Glasgow, 1984.